Development of a New Gravitational Geoid Model for Japan

Koji MATSUO, Takayuki MIYAZAKI, Yuki KUROISHI, Japan

Key words: Geoid modeling, Height Reference System, Gravity

SUMMARY

We develop an improved gravitational geoid model for Japan by incorporating up-to-date Global Gravity Model (GGM) from GOCE satellite, marine gravity data from satellite altimetry, and terrestrial gravity data. The strategy for modelling of gravitaitonal geoid is based on Remove-Compute-Restore technique with Helmert's second method of condensation, which is the same approach as the previous model by Kuroishi (2009). First, we investigate the impacts of the newly adopted GGMs on geoid determination by experimenting with nine GGMs published in recent years. Based on the result, we employ GO_CONS_GCF_2_DIR_R5 model [Bruinsma et al., 2013] as GGM. Next, we update marine gravity data. Here we use the altimetry-derived marine gravity data instead of the shipborne data because the shipborne data is known to contain a large number of outliers [Kuroishi & Keller, 2005]. We adopt Global Marine Gravity model v23.1 from Cryosat-2 & JASON-1 satellites provided by Sandwell et al. (2014). Last, we incorporate about 290,000 of the terrestrial gravity data. As a consequent, we have succeeded to create the Japanese gravitational geoid model with an accuracy of 7.8 cm in the standard deviation compared with GNSS/Leveling geoid undulations, which is improved by 0.6 cm in the standard diviation as compared to the previous model.

Development of a New Gravitational Geoid Model for Japan

Koji MATSUO, Takayuki MIYAZAKI, Yuki KUROISHI, Japan

1. INTRODUCTION

The geoid is the equipotential surface that corresponds to global average sea surface. Currently, there are two geodetic approaches to determine geoid undulation. One approach is the direct measurement by spirit leveling and Global Navigation Satellite System (GNSS) positioning. Combination of spirit leveling and gravimetry provides relative difference of physical orthometric height, while GNSS positioning does geometorical ellipsoidal height. Geoid height can be derived from the subtraction of orthometric height from ellipsoidal height [e.g. Heiskanen and Moriz, 1967]. This approach is termed "GNSS/leveling method". GNSS/leveling method enables a high-presition measurement of geoid height over short distance. However, it is difficult to cover long distances because spirit leveling is time-consuming and suffers from cumulative errors in proportion to distance. The other approach is computational modeling based on gravity data. Geoid height can be computed with global integration of gravity anomalies which is measurable via terrestrial and satellite gravimetry. This approach is termed "Gravimetric approach". Gravimetric approach is more efficient than GNSS/leveling method because gravity anomaly is comparatively easy to efficiently measure wide area with high spatial resolution. However, this approach requires complicated calculations.

Geoid models are commonly used to transform GNSS-derived ellipsoidal height to orthometric height [e.g. Featherstone, 2001]. At present, GNSS technique has successfully matured and has achieved a high-precision measurement of ellipsoidal height with several centimeter accuracy. Therefore, if a well-determined geoid model is given, one can precisely derive orthometric height from GNSS positioning, and furthermore establish a reference height system from GNSS instead of spirit leveling. The present height reference systems in the world including Japan are mostly based on spirit leveling, whose benchmarks are connected to single or multiple tide gauge stations that measure local mean sea level as the reference surface for the system. As described above, an enormous task is required to keep measuring the height of all benchmarks by spirit leveling. Accordingly, increasing efforts are being made to establish the geoid-based height reference systems in many countries. For examples, National Geodetic Survey of the United States started a project named GRAV-D in 2012 to realize the geoid-based height reference system for 10 countries around North America [Smith and Roman, 2010] (The details can be found in http://www.ngs.noaa.gov/GRAV-D/pubs/GRAV-D_v2007_12_19.pdf). Likewise, several countries in Asia have conducted airborne gravimetry and attempted to construct the geoid-based height reference system [e.g. Forsberg et al., 2007: Hwang et al., 2007].

Japan is also considering to establish its height reference system based on geoid. In order to achieve this, it is absolutely essential to develop a high-precision geoid model. Regional gravimetric geoid model for Japan has been developed by Geospatial Information Authority of Japan (GSI) [e.g. Kuroishi, 1995; Kuroishi & Keller 2005]. The latest model named “JGEOID2008” is constructed by applying Remove-Compute-Restore (RCR) techniques under the assumption of Helmert’s second method of condensation (Stokes-Helmert scheme) [Kuroishi, 2009]. This model incorporates the Global Geopotential Model (GGM) from GRACE satellites [Tapley et al., 2005], 260,000 of the terrestrial gravity data, and 580,000 of the shipborne gravity data for sea and ocean surrounding Japan. As a consequence, JGEOID2008 is consistent with the GNSS/Leveling-derived geoid heights at 816 benchmarks within 10 cm in the standard deviation.

With the successful operation of the dedicated satellite gravimetry mission GOCE during 2009-2013, a number of GGMs with high accuracy and spatial resolution has been available. Utilization of such data will improve the performance of gravimetric geoid model. In this paper, we attempt to develop an improved gravimetric geoid model of Japan by employing up-to-date gravity data including GOCE data. The strategy for constructing the gravimetric geoid model is the same as the previous work by Kuroishi (2009), i.e. the RCR technique using Stokes-Helmert scheme. First, we update the GGM. We experiment with nine GGMs published in recent years and select the best GGM to minimize the standard deviation of difference with the geoid heights measured by GNSS/Leveling method. Next we update marine gravity data. Here we adopt Global Marine Gravity model v23.1 from Cryosat-2 & JASON-1 satellites provided by Sandwell et al. (2014). Last, we incorporate 290,000 of terrestrial gravity data, which is 30,000 more than the previous work. Finally, we evaluate the performane of the newly developed gravitational gravity model by comparing with the geoid heights measured by GNSS/Leveling method at 971 benchmarks. The geographical map of GNSS/leveling geoid heights is shown in Fig.1.

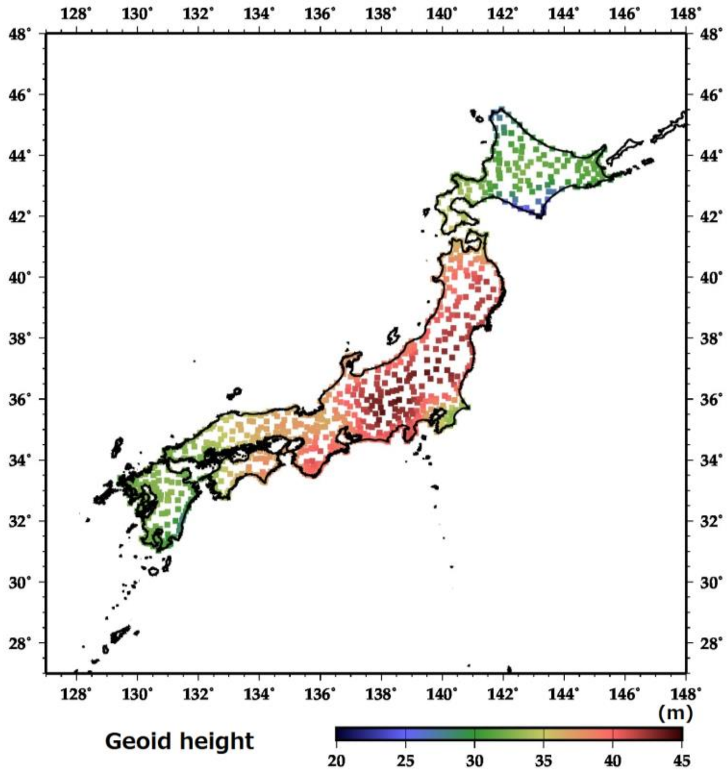

Fig. 1 GNSS/leveling geoid heights at 971 benchmarks.

2. THEORY

Here the RCR techniques with Stokes-Helmert scheme is employed to construct the gravitational geoid model. The details on this scheme can be found in many papers [e.g. Vanicék and Martinec,1994]. The basic equation is expressed as follow:

$$N = N_{GGM} + N_{res} + N_{ind} \tag{1}$$

where N is the geoid height, N_{GGM} is the GGM-derived geoid height, N_{res} is the residual geoid height, and N_{ind} is the indirect effect. N_{GGM} reflects the long-wavelength feature of geoid undulation, while N_{res} does the medium and short wavelength feature. N_{ind} is a term for correcting for the bias between the obtained geoid and real geoid, which is caused by the assumption that topographic mass outside the geoid is condensed onto the geoid.

3. SELECTION OF GGM

In general, GGMs are provided in the form of spherical harmonic coefficients (Stokes coefficients). The geoid height is computed from GGM's Stokes coefficients using the following equation:

$$N_{GGM} = N_0 + \frac{GM}{r\gamma} \sum_{n=2}^{n_{max}} \left(\frac{a_{GGM}}{r}\right)^n \sum_{m=0}^{n} (\overline{C'}_{nm} \cos m\varphi + \bar{S}_{nm} \sin m\varphi) \bar{P}_{nm} (\cos\theta), \tag{2}$$

where N_0 is the zero degree term, GM is the product of the universal gravitational constant and the Earth's mass of GGM, (r,□□□□□ are the spherical polar coordinates (geocentric radius, latitude, longitude) of the computation point, □ is the normal gravity of the Geodetic Reference System (GRS) 80 ellipsoid [Moritz, 1980], a_{GGM} is the scaling parameter of GGM, n and m are the degree and order of Stokes coefficients, n_{max} is the maximum degree of GGM, $\overline{C'}_{nm}$ and $\bar{S}_{nm}$ are the 4□ normalized Stokes coefficients after subtracting the even zonal harmonics of the GRS80 ellipsoid, $\bar{P}_{nm}$ is the 4□ normalized Legendre functions. The zero degree term N_0 is given as,

$$N_0 = \frac{GM - GM_0}{R\gamma} - \frac{W_0 - U_0}{\gamma}, \tag{3}$$

where GM_0 is the product of the universal gravitational constant and the Earth's mass of the GRS80 ellipsoid, R is the spherical Earth radius, W_0 is the gravity potential of the geoid, and U_0 is the normal gravity potential of the GRS80 ellipsoid. Here we used W_0 value of 62,636,853.4 m^2s^{-2} [IAG, 2015].

The GGMs evaluated here are the following nine models: GGM02S model [Tapley et al., 2005], GGM05S model [Tapley et al., 2013], ITG-Goce02 model [Schall et al., 2014], JYY_GOCE04S model [Yi et al., 2013], GOGRA04S model [Yi et al., 2013], GGM05G model [Bettadpur et al., 2015], EIGEN6S2 model [Rudenko et al., 2014], GOCO05s model[Mayer-Gürr et al., 2015], GO_CONS_GCF_2_DIR_R5 model [Bruinsma et al., 2013]. All models are publically available at the International Centre for Global Earth Models (ICGEM) [Barthelmes & Kohler, 2012]. The overview on these models is summarized in Table 1.

Figure 2 displays the geographical maps of geoid undulation in and around Japan using each GGM. We evaluated them by comparing with those measured by GNSS/leveling method at 971 benchmarks. We computed the standard deviations of difference between GGM-derived geoid heights and GNSS/leveling-derived geoid heights. Table 2 represents the statistics of the standard deviations. As shown in Table 2, GO_CONS_GCF_2_DIR_R5 model showed the smallest standard deviation among the all GGMs. Thus, we adopted GO_CONS_GCF_2_DIR_R5 model as GGM.

Table 1 Overview of the GGMs evaluated in this study. All models can be download from the ICGEM website (http://icgem.gfz-potsdam.de/ICGEM/).

GGM model	Maximum degree	Satellite data
GGM02S [Tapley et al., 2005]	160	GRACE (2002 Apr. - 2003 Dec.)
GGM05S [Tapley et al., 2013]	180	GRACE (2003 Mar. - 2013 May)
ITG-Goce02 [Schall et al., 2014]	240	GOCE (2009 Nov. - 2010 Jun.)
JYY_GOCE04S [Yi et al., 2013]	230	GOCE (2009 Nov. - 2013 Oct.)
GOGRA04S [Yi et al., 2013]	230	GRACE (2002 Aug. - 2009 Aug.) GOCE (2009 Nov. - 2013 Oct.)
GGM05G [Bettadpur et al., 2015]	240	GRACE (2003 Mar. - 2013 May) GOCE (2009 Nov. - 2013 Oct.)
EIGEN6S2 [Rudenko et al., 2014]	260	SLR (1985 - 2010) GRACE (2003 Oct. - 2012 Sep.) GOCE (2009 Nov. - 2013 May.)
GOCO05s [Mayer-Gürr et al., 2015]	280	SLR (1985 - 2010) GRACE (2003 Feb. - 2013 Dec.) GOCE (2009 Nov. - 2013 Oct.)
GO_CONS_GCF_2_DIR_R5 [Bruinsma et al., 2013]	300	SLR (1985 - 2010) GRACE (2003 - 2012) GOCE (2009 Nov. - 2013 Oct.)

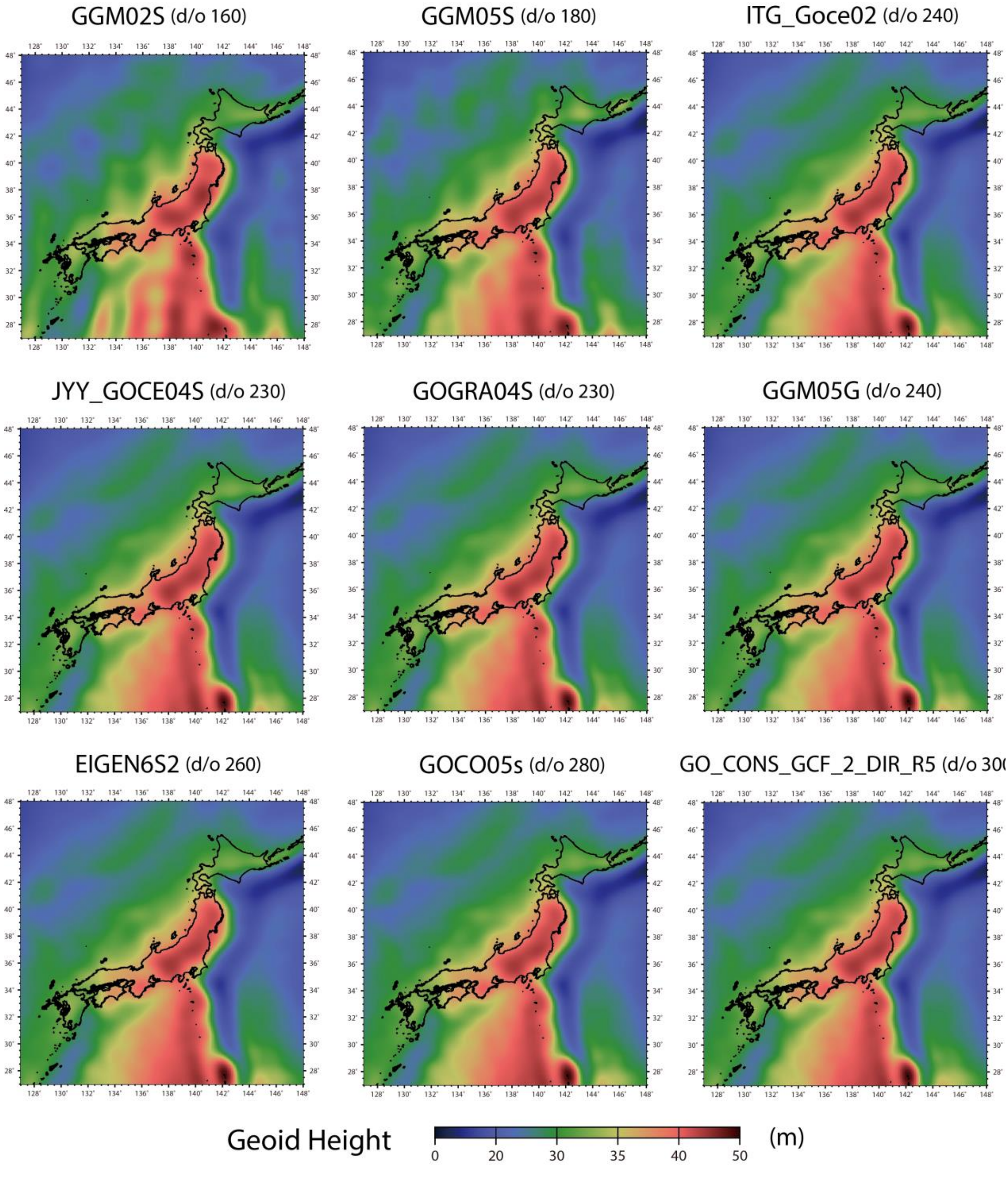

Fig. 2 Geoid undulations in and around Japan derived from nine GGMs.

Table 2 Statistics of standard deviation (SD) of difference between each GGM-derived geoid height and GNSS/leveling-derived geoid height.

GGM model	SD (Unit: cm)
(Degree and Order up to 160)	
GGM02S	100.59
GGM05S	85.38
ITG-Goce02	82.95
JYY_GOCE04S	83.13
GOGRA04S	83.16
GGM05G	83.11
EIGEN6S2	83.24
GOCO05s	83.16
GO_CONS_GCF_2_DIR_R5	83.23
(Degree and Order up to 180)	
GGM05S	75.12
ITG-Goce02	65.67
JYY_GOCE04S	65.18
GOGRA04S	65.17
GGM05G	65.34
EIGEN6S2	65.26
GOCO05s	64.99
GO_CONS_GCF_2_DIR_R5	65.12
(Degree and Order up to 200)	
ITG-Goce02	57.30
JYY_GOCE04S	57.04
GOGRA04S	57.05
GGM05G	57.05
EIGEN6S2	57.05
GOCO05s	56.82
GO_CONS_GCF_2_DIR_R5	56.82

GGM model	SD (Unit: cm)
(Degree and Order up to 220)	
ITG-Goce02	54.64
JYY_GOCE04S	55.23
GOGRA04S	55.21
GGM05G	55.03
EIGEN6S2	55.29
GOCO05s	54.66
GO_CONS_GCF_2_DIR_R5	54.70
(Degree and Order up to 240)	
ITG-Goce02	53.03
GGM05G	50.92
EIGEN6S2	51.63
GOCO05s	50.34
GO_CONS_GCF_2_DIR_R5	50.38
(Degree and Order up to 260)	
EIGEN6S2	49.44
GOCO05s	46.32
GO_CONS_GCF_2_DIR_R5	47.07
(Degree and Order up to 280)	
GOCO05s	45.38
GO_CONS_GCF_2_DIR_R5	45.91
(Degree and Order up to 300)	
GO_CONS_GCF_2_DIR_R5	45.05

4. RESIDUAL GEOID HEIGHT N_{RES}

The residual geoid height can be computed as follows:

$$N_{res} = \frac{R}{4\pi\gamma} \iint_{\sigma_0} (\Delta g_F - \Delta g_{GGM}) S(\psi) d\sigma \tag{4}$$

where σ_0 is the integration area, Δg_F is the faye gravity anomaly from terrestrial gravity data [Wang and Rapp, 1990], Δg_{GGM} is the free-air gravity anomaly derived from GGM, $S(\psi)$ is the spherical Stokes kernel, ψ is the angular distance between the computation point and terrestrial gravity data, $d\sigma$ is the surface element.

The faye gravity anomaly Δg_F is computed from terrestrial gravity data using the following equation:

$$\Delta g_F = FA + AC + TC \tag{5}$$

where *FA* is the free-air gravity anomaly from terrestrial gravity data, *AC* and *TC* are the atmospheric and terrain gravity correction, respectively. The free-air gravity anomaly *FA* and atmospheric gravity correction *AC* are computed using the relationships proposed by Heiskanen and Moriz (1967) and Wichiencharoen (1982):

$$\begin{aligned} FA = g_{obs} - \gamma_\theta & \\ + \gamma_e\big[\{1 + f + m - (3f - 5m/2)\sin^2\theta\}(2H_p/a) & \\ - (3H_p/a)^2\big] & \end{aligned} \tag{6}$$

$$AC = 0.8658 - 9.727 \cdot 10^{-5} H_p + 3.482 \cdot 10^{-9} H_p^2 \tag{7}$$

where g_{obs} is the gravity values observed by terrestrial gravimetry, γ_θ and γ_e are the normal gravity at latitude θ and the equator, *f* is the polar flattening of the GRS80 ellipsoid, *a* is the length of semi-major axis of the GRS80 ellipsoid, H_p is the orthometric height at a computation point. *m* is the ratio of centrifugal forces and gravitational coefficient which is given as,

$$m = \frac{\omega^2 a^3 b}{GM} \tag{8}$$

where ω is the angular velocity from the GRS80 ellipsoid, *b* is the length of semi-minor axis of the GRS80 ellipsoid. Unit of *AC* and *H* are mili-Gal and meter, respectively. The terrain gravity correction *TC* is calculated based on a spherical approximation proposed by Martinec and Vanicék (1994a) of the geoid:

$$TC = -\frac{4\pi G\rho_0}{R}H_p^2 + \frac{G\rho_0 R^2}{2}\iint_{\sigma_1}\frac{H^2 - H_p^2}{l^3}(1 - \frac{3H_p^2}{l^2})d\sigma + \frac{G\rho_0 R^2}{2}\iint_{\sigma_2}\frac{H^2 - H_p^2}{l_0^3}(1 - 3\,sin^2\frac{\psi}{2})d\sigma \tag{9}$$

where □$_0$ is the topographic density (2670 kg/m^3), H is orthometric height at running points, σ_1 and σ_2 are a near zone and a far zone of integration area. l and l_0 are the spatial distances between computation point and running points which are given as:

$$l = \left[\left(R + H_p\right)^2 + R^2 - 2(R + H_p)R\cos\psi\right]^{\frac{1}{2}}, \tag{10}$$

$$l_0 = 2R\sin\frac{\psi}{2}. \tag{11}$$

The near-zone is defined as the area within the spherical distance □□□given as [Martinec and Vanicék, 1994a],

$$\psi_0 = \sqrt{\frac{H_p}{R}}. \tag{12}$$

GGM-derived free-air gravity anomaly Δg_{GGM} is computed from terrestrial gravity data using the following equation:

$$\Delta G_{GGM} = g_0 + \frac{GM}{r^2}\sum_{n=2}^{n_{max}}(n-1)\left(\frac{a_{GGM}}{r}\right)^n\sum_{m=0}^{n}(\overline{C'}_{nm}\,cos\,m\varphi + \bar{S}_{nm}\,sin\,m\varphi)\bar{P}_{nm}\,(cos\,\theta). \tag{13}$$

g_0 is the zero degree term which is computed using the following equation:

$$g_0 = -\frac{GM - GM_0}{R^2} + \frac{2(W_0 - U_0)}{\gamma}. \tag{14}$$

In order to obtain the residual geoid height, we used the following data sets: terrestrial gravity data, marine gravity data, digital elevation model (DEM), and GGM. The terrestrial gravity data are collected from the database constructed by research institutes and universities in Japan. GSI has established the gravity reference network for Japan in 1950s and provides 16,441 of terrestrial gravity data. Geological Survey of Japan (GSJ) constructed the gravity database named 'GALILEO' and provides 173,365 of terrestrial gravity data [GSJ, 2013]. Yamamoto et al. (2011) published the gravity database of southwest Japan and provides 73,304 of terrestrial gravity data. Kanazawa university and Hokkaido university also have their own gravity database and provides 26,915 of terrestrial gravity data [Honda et al., 2013]. As a result, we collected 290,025 of terrestrial gravity data in total. Direct terrain effect shown in Eq.(9) is derived from DEM. DEM of Japan is created by GSI based on airborne digital photography and laser altimetry. We here used 9 second (~250m) DEM. As for marine gravity data, about 580,000 of shipborne data are available. However, the shipborne data is known to contain a large number of outliers [Kuroishi & Keller, 2005]. Thus, we used Global Marine Gravity model v23.1 from Cryosat-2 & JASON-1 satellites provide by Sandwell et al. (2014) instead of the shipborne data. Using these data set, faye gravity anomaly and GGM-derived gravity anomaly are calculated. The residual gravity anomaly obtained is interpolated into 1×1.5 arc-minute grid by Kriging technique. Figure 3 displays the geographical map of residual gravity anomaly.

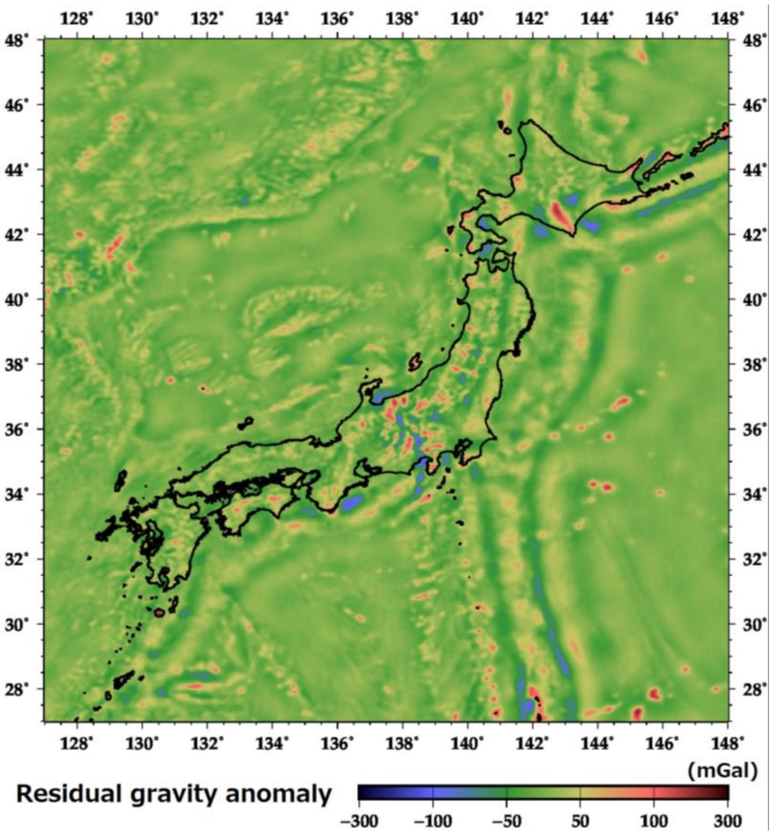

Fig. 3 Residual gravity anomaly in and around Japan.

Next, we convert the residual gravity anomaly into the residual geoid height by stokes integration. In order to alleviate the truncation error, we adopted the hybrid-Molodensky modified spheroidal Stokes kernel proposed by Featherstone et al. (1998). The optimal spherical cap size and modification of degree were determined by performing grid search to minimize the difference with GNSS/leveling geoid height whose long-wavelength component was removed by GGM. The residual geoid height obtained is shown in Figure 4. The maximum value of residual geoid height is 2.79 m and the minimum values is -1.59m.

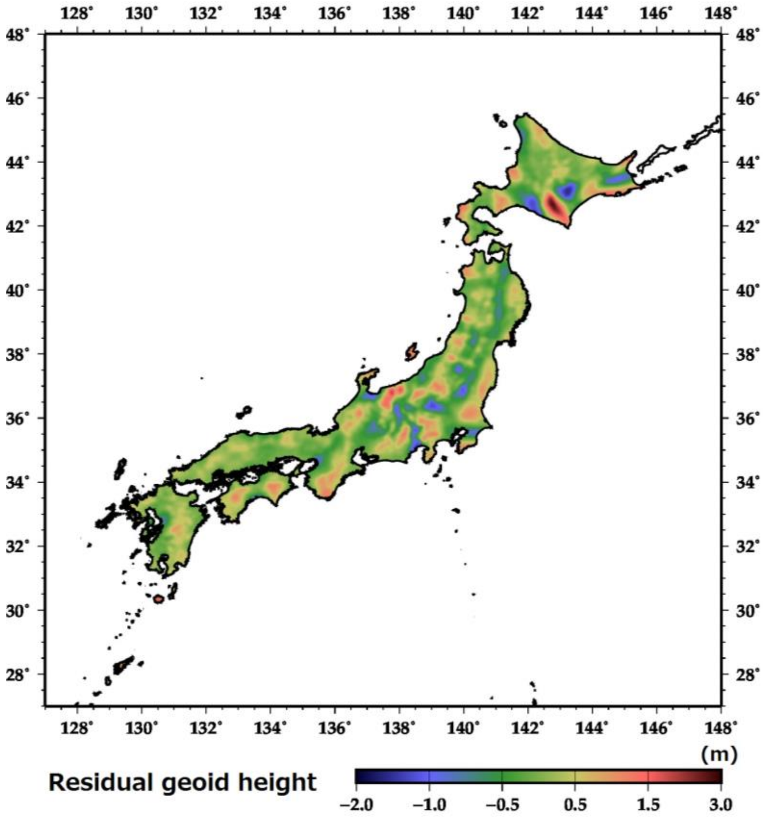

Fig. 4 Residual geoid height for Japan.

5. INDIRECT EFFECT N_{IND}

The Stokes-Helmert scheme does not produce the geoid but the cogeoid because the topographic mass outside the geoid is condensed onto the geoid. Such discrepancy between the geoid and cogeoid is called indirect effect. This can be computed from DEM using the following equation [Martinec and Vanicék, 1994b]:

$$N_{ind} = -\frac{2\pi G\rho_0}{\gamma} H_p^2 + \frac{G\rho_0 R^2}{\gamma} \iint_\sigma \left[2\frac{\sqrt{l^2+H^2} - \sqrt{l^2+H_p^2}}{R} + \ln \frac{\frac{l}{2R} + H + \sqrt{l^2+H^2}}{\frac{l}{2R} + H_p + \sqrt{l^2+H_p^2}} - \frac{H-H_p}{l} \right] d\sigma \,. \tag{15}$$

The spherical effect of topography is taken into account in this equation. The geographical map of indirect effect N_{ind} obtained is shown in Figure 5. The maximum value of N_{ind} is 0.01 m and the minimum is -1.49 m. Large indirect effect can be found in the area with high topographic relief.

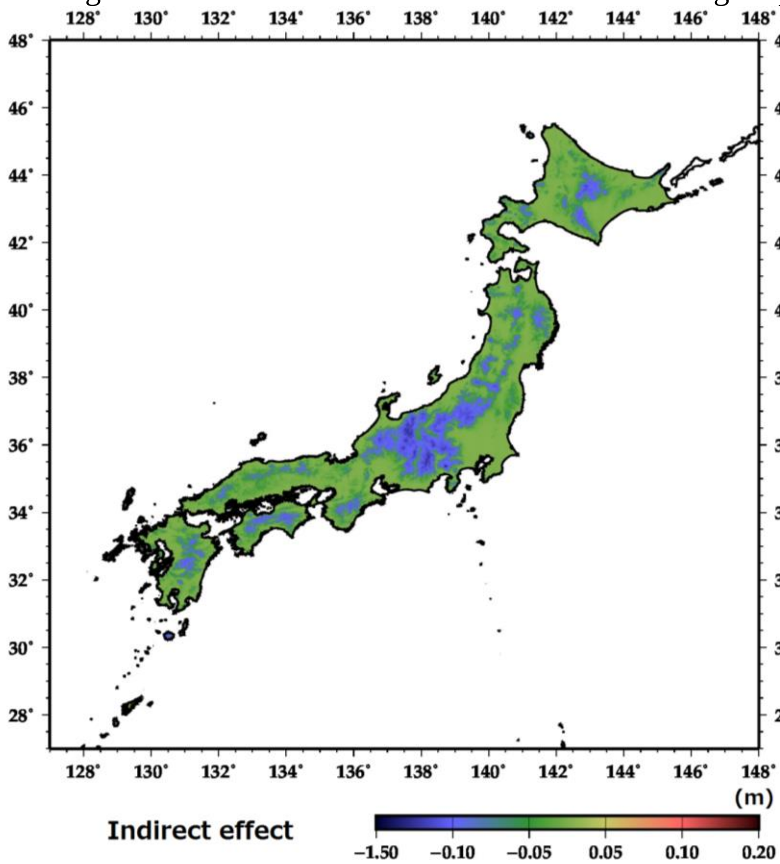

Fig. 5 Indirect effect on geoid over Japan

6. GRAVITATIONAL GEOID MODEL OF JAPAN

In Stokes-Helmert scheme, gravitational geoid model is divided into three components (N_{GGM}, N_{res}, and N_{ind}) as shown in Eq. (1). The gravitational geoid model is restored by summing the divided three components (Fig. 2, Fig.4, and Fig. 5). The geographical map of the gravitational geoid height constructed by this study is represented in Figure 6. The maximum value of geoid height is 47.43 m and the minimum value is 19.49 m. The standard deviation of difference between this model and GNSS/leveling geoid height is 7.8 cm. Thus a slight improvement in standard deviation is confirmed as compared to the previous geoid model (JGEOID2008) whose standard deviation is 8.4 cm. It appears that the incorporation of GOCE-derived GGM contributes to the improvement of the gravitational geoid model to a large extent.

The difference between GNSS/leveling geoid height and gravimetric geoid model is mapped in Figure 7. Overall the trend, northeastern part of Japan (Hokkaido and Tohoku regions) is biased to negative, while southwestern part (Kansai, Chugoku, Kyushu regions) positive. Such apparent slope is also found in other countries and can be attributed to the ocean's time-mean dynamic topography (MDT) [e.g. Featherstone & Filmer, 2012]. When this oceanic effect is corrected for GNSS/leveling geoid height using MDT model, the standard deviation of difference is expected to be reduced. This is one of the subjects for our future study.

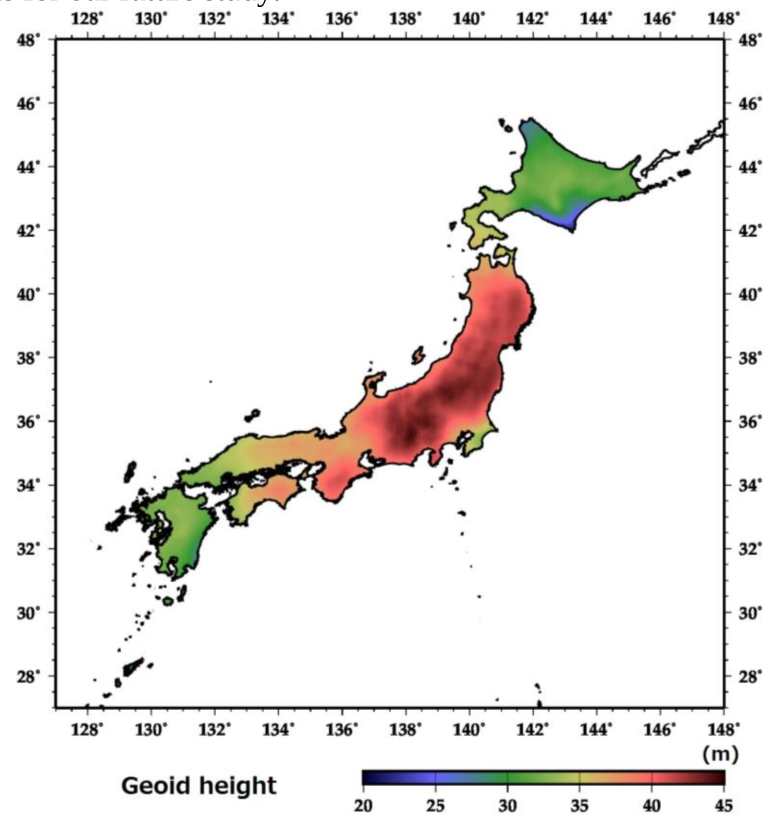

Fig. 6 Gravimetric geoid model constructed by this study.

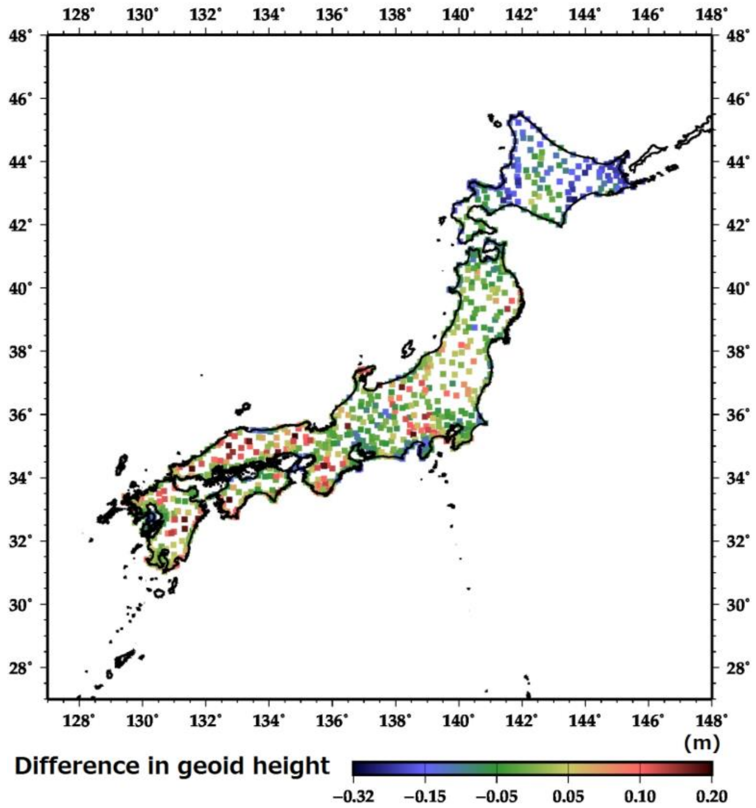

Fig. 7 Difference between GNSS/leveling geoid height and gravimetric geoid model.

7. SUMMARY AND FUTURE PERSPECTIVE

In this study, we developed a new gravimetric geoid model of Japan based on Stokes-Helmert scheme. The point for improvement is to incorporate the up-to-date gravity data such as GOCE-derived GGM and altimetry-derived marine gravity data. At the beginning, we investigated the performance of the recently released GGMs by comparing the GGMs with GNSS/leveling geoid heights. We found that GO_CONS_GCF_2_DIR_R5 model was the best model in this case. Using this model, we computed the long-wavelength component of geoid undulation and free-air gravity anomaly. Next, we calculated the residual geoid height using terrestrial gravity data, marine gravity data, GGM, and DEM. The modified stokes kernel proposed by Featherstone et al. (1998) is applied to global integration of the residual gravity anomaly in order to reduce the truncation error. The indirect effect is derived from DEM based on a spherical approximation. By summing GGM-derived geoid height, the residual geoid height, and the indirect effect, we constructed gravimetric geoid model of Japan as shown in Figure 6. At the final stage, we evaluated the performance of our gravimetric geoid model by comparing with GNSS/leveling geoid heights. Then we obtained the standard deviation of 7.8 cm, which is improved by 0.6 cm in comparison with the previous geoid model.

Although we succeeded in improving gravimetric geoid model of Japan, there is room for further improvement. For example, the terrain effect can be more rigorously calculated because more accurate DEM with 0.3 arc second (10m) resolution, which is provided by GSI, is already available. Such high resolution DEM is also useful to construct the residual terrain model [e.g. Forsberg, 1984], which can complement the short-wavelength component of geoid undulation. The lateral and radial topographic density model also enables accurate determination of the terrain effect and the residual terrain model, improving the performance of gravimetric geoid model. In addition, the alternative strategies for geoid modeling such as Molodensky scheme [Molodensky et al., 1962] or KTH method [Sjöberg, 2003] are expected to improve gravimetric geoid model. In the future, we are going to experiment with these strategies and attempt to further improve gravimetric geoid model of Japan.

REFERENCES

Barthelmes, F. & Kohler, W., 2012 International Centre for Global Earth Models (ICGEM), Journal of Geodesy, The Geodesists Handbook 2012, 86(10), 932-934.

Bettadpur S, Ries J, Eanes R, Nagel P, Pie N, Poole S, Richter T, and Save H (2015) Evaluation of the GGM05 Mean Earth Gravity models, Geophysical Research Abstracts, Vol. 17, EGU2015-4153.

Bruinsma S, Foerste C, Abrikosov O, Marty JC, Rio MH, Mulet S, Bonvalot S (2013) The new ESA satellite-only gravity field model via the direct approach, Geophys. Res. Lett. 40, 14, 3607-3612. doi:10.1002/grl.50716

Featherstone WE, Evans JD, Olliver JG (1998) A Meissl-modified Vanicék and Kleusberg kernel to reduce the truncation error in gravimetric geoid computations, Journal of Geodesy 72(3), 154-160.

Featherstone WE (2001) Absolute and relative testing of gravimetric geoid models using global positioning system and orthometric height data, Computers & Geosciences 27(7), 807-814.

Featherstone WE and Filmer MS (2012) The north-south tile in the Australian Height Datum is explained by the ocean's mean dynamic topography, J. Geophys. Res., 117, C08035, doi:10.1029/2012JC007974

Forsberg R (1984) A study of terrain reductions, density anomalies and geophysical inversion methods in gravity field modeling, Report 355, Department of Geodetic Science and Surveying, Ohio State University, Columbus, USA

Forsberg R, Olesen A, Munkhtsetseg D and Amarzaya B (2007) Downward continuation and geoid determination in Mongolia from airborne and surface gravimetry and SRTM topography, International Forum on Strategic Technology

Geological Survey of Japan (eds.) (2013) Gravity Database of Japan. DVD edition, Digital Geoscience Map P-2, Geological Survey of Japan, AIST

Heiskanen WA and Moritz H (1967) Physical Geodesy, W.H. Freeman and Co., San Francisco

Honda R, Sawada A, Furuse N, Kudo T, Tanaka T, Hiramatsu Y (2013) Release of Gravity Database of the Kanazawa University, Journal of the Geodetic Society of Japan, 58(4), 153-160

Hwang C, Hsio YS, Shih HC, Yang M, Chen KH, Forsberg R and Olesen A (2007) Geodetic and geophysical results from a Taiwan airborne gravity survey: Data reduction and accuracy assessment, J Geophys. Res., 112, B04407, doi:10.1029/2005JB004220

IAG (2015) IAG Resolution (No. 1) for the definition and realization of an International Height Reference System (IHRS), http://iag.dgfi.tum.de/fileadmin/IAG-docs/IAG_Resolutions_2015.pdf

Kuroishi Y (1995) Precise gravimetric determination of geoid in the vicinity of Japan, Bull. Geogr. Surv. Inst., 41, 1-93

Kuroishi Y and Keller W (2005) Wavelet approach to improvement of gravity field-geoid modeling for Japan, J. Geophys. Res., 110, B03402

Kuroishi Y (2009) Improved geoid model determination for Japan from GRACE and a regional gravity field model, Earth Planets Space, 61, 807-813

Sandwell DT, Muller RD, Smith RHF, Garcia E, Francis R (2014) New global marine gravity model from CryoSat-2 and Jason-1 reveals buried tectonic structure, Science, 346, 65-67

Schall J, Eicker A, Kusche J (2014) The ITG-Goce02 gravity field model from GOCE orbit and gradiometer data based on the short arc approach, Journal of Geodesy, Volume 88, Issue 4, pp 403-409, doi:10.1007/s00190-014-0691-2

Smith DA and Roman DR (2010) How NOAA's GRAV-D project impacts and contributes to NOAA science. http://www.ngs.noaa.gov/GRAV-D/pubs/GRAV-D_Contribution_to_NOAA_Science.pdf (accessed at March 24, 2016)

Sjöberg LE (2003) A computational scheme to model geoid by the modified Stokes formula without gravity reductions. Journal of Geodesy, 74:255-268.

Tapley BD, Ries J, Bettadpur SV, Chambers D, Cheng MK, Condi F, Gunter B, Kang Z, Nagel P, Pastor R, Pekker T, Poole S and Wang F (2005) GGM02C - An improved Earth gravity field model from GRACE. Journal of Geodesy, Vol. 79, No. 8, pp. 467-478, doi: 10.1007/s00190-005-0480-z

Tapley BD, Flechtner F, Bettadpur SV, Watkins MM (2013) The status and future prospect for GRACE after the first decade, Eos Trans., Fall Meet. Suppl., Abstract G22A-01

Martinec Z and Vanicék P (1994a) Direct topographical effect of Helmert's condensation for a spherical approximation of the geoid, Manuscripta geodaetica, Vol. 19, pp257-268

Martinec Z and Vanicék P (1994b) The indirect effect of topography in the Stokes-Helmert technique for a spherical approximation of the geoid, Manuscripta geodaetica, Vol. 19, pp213-219

Mayer-Gürr T, et al. (2015): The combined satellite gravity field model GOCO05s. Presentation at EGU 2015, Vienna, April 2015.

Molodensky MS, Eremeev VF, Yurkina MI, (1962) Methods for study of the external gravitational field and figure of the Earth. Translated from Russian by the Israel program for scientific translations, Office of Technical Services Department of Commerce, Washington, D.C.

Moritz (1980) Geodetic Reference System 1980, Bulletin Geodesique, Vol. 54, No. 3, pp.395-405, doi:10.1007/BF02521480

Rudenko S., Dettmering D., Esselborn S., Schoene T., Foerste C., Lemoine J. M., Ablain M., Alexandre D., Neumayer K. H. (2014) Influence of time variable geopotential models on precise orbits of altimetry satellites, global and regional mean sea level trends. Advances in Space Research, doi: 10.1016/j.asr.2014.03.010

Vanicék P. and Martinec Z. (1994) The Stokes-Helmert scheme for the evaluation of a precise geoid. Manuscripta Geodaetica 19: 119-128

Yamamoto A., Shichi R and Kudo T (2011) Gravity Measurements and Database in Japan, Gravity Database of Japan (CD-ROM), Earth Watch Safety Net Research Center, Chubu University, Special Publication, No.1

Yi W., Rummel R., Gruber T. (2013) Gravity field contribution analysis of GOCE gravitational gradient components. Studia Geophysica et Geodaetica, p174-202, doi:10.1007/s11200-011-1178-8

Wang Y. M. and Rapp RH (1990) Terrain Effects on Geoid Undulation Computation, man. geod., 15, 23-29

Wichiencharoen (1982) Fortran program for computing geoid undulations from potential coefficients and gravity anomalies. Internal Report, Department of Geodetic Science and Surveying, Ohio State University, Columbus, USA

BIOGRAPHICAL NOTES

Koji Matsuo is a researcher of the Geography and Crustal Dynamics Research Center, Geospatial Information Authority of Japan, Tsukuba, Japan. His current research interests include satellite gravimetry and its application to earth science. He received his M. Sc. and D. Sc. degree in Geophysics from Hokkaido University, Sapporo, Japan in 2010 and 2013.

CONTACTS

Koji Matsuo
Geospatial Information Authority of Japan
Kitasato 1, Tsukuba, Ibaraki
JAPAN
Tel. +81-29-864-4767
Fax + 81-29-864-1802
Email: matsuo-k96s4@mlit.go.jp
Web site: http://www.gsi.go.jp/ENGLISH/index.html